ELSEVIER

Contents lists available at ScienceDirect

## **Extreme Mechanics Letters**

journal homepage: www.elsevier.com/locate/eml



## Passive nonreciprocity-induced directional wave scattering



Department of Mechanical and Aerospace Engineering, Rutgers University, Piscataway, NJ 08854-8058, USA



#### ARTICLE INFO

Article history:
Received 18 September 2021
Received in revised form 10 December 2021
Accepted 23 December 2021
Available online 30 December 2021

Keywords: Wave directivity Bilinear stiffness Spatial asymmetry 2D lattice Nonreciprocity Waveguide

#### ABSTRACT

Controllable nonreciprocal wave redirection in two dimensions is demonstrated by a monatomic lattice of masses and nonlinear springs. The key is a functional section with a spatially asymmetric arrangement of bilinear stiffness. Regardless of the external force driving frequency or the location of the source relative to the functional section, a stable effect is obtained showing scattered wave motion towards two opposite directions each with oppositely signed displacement offsets. Crucially, the bilinear nature of the springs, with linear response but different stiffness coefficients in compression and tension, makes the passive nonreciprocal redirection effect independent of signal amplitude. Consistent nonreciprocal scattering is demonstrated first for a lattice section with asymmetrically distributed bilinearity. Combinations of these fundamental lattice sections with modified bilinear stiffness and orientation of the asymmetric arrangement demonstrate a wide variety of directional scattering effects, illustrating an ability to control the preferred propagating directions and the signs of the dynamic displacement offsets. These results suggest a novel type of nonreciprocal 2D waveguide whose underlying nonlinear mechanism is fundamentally different from actively-achieved alternative methods such as topologically protected edge states.

© 2021 Elsevier Ltd. All rights reserved.

#### 1. Introduction

Strongly anisotropic and *reciprocal* dynamic effects with wave propagation restricted to certain directions are possible in passive linear two-dimensional (2D) periodic structures [1,2]. The challenge is to achieve tunable *nonreciprocal* wave directivity that breaks the limitation arising from the reciprocal nature of linearity. Generally speaking, two different methods have been proposed to realize nonreciprocal propagation: active approaches using energy input and passive approaches based on nonlinearity.

Active methods employ topologically protected edge states (TPESs), a phenomenon found in many 2D one-way propagating systems [3]. TPESs occur at the shared boundary of two lattice structures, across which topology changes and the system is forced to close its bandgap locally in support of localized edge states, so that the shape of the interface decides the pathway of wave motion and becomes immune to scattering into the main bodies of these sections. Nonreciprocal topologically protected wave propagation can be realized actively by the introduction of gyroscopic [4,5] and fluid flow effects [6,7].

Current passive methods depend solely on weak nonlinearity that perturbs dispersion surfaces in terms of amplitude, and therefore remain reciprocal. For example, replacing linear springs with nonlinear ones having cubic stiffness coefficients makes a

\* Corresponding author. E-mail address: zhaocheng.lu@rutgers.edu (Z. Lu). non-propagating wave become propagating, or vice versa [2,8]. Passive nonreciprocal models necessarily require spatially asymmetric nonlinearity, and can achieve significant control over wave propagation, e.g., one-way propagation in 1D [9-14] and 2D [15] scenarios. Compared to the active methods that require external energy input and can be inherently unstable, passive methods have zero energy cost and are easily controlled. In this work we propose a novel approach to control 2D wave directionality by taking advantage of a passive nonreciprocity; the main idea is to generate the dominant propagation directions via bilinear springs, a special form of nonlinearity. Bilinearity is a unique type of non-perturbative nonlinearity that maintains the linear property of amplitude independence, meaning that a scaling of the input leads to the same output signal scaled by the input amplification factor. This phenomenon is common in different engineering scenarios. Continuous materials with bilinear constitutive elastic behavior (also known as heteromodular or bimodular in continuum mechanics) have been proposed as nonlinear models for contact forces [16], elastic solids containing cracks [17], and for the dynamics of geophysical systems, including granular media [18]. Wave motion in bimodular media has been studied extensively [19-28]. Recent studies have shown that wave motion in discrete spring-mass chain systems with bilinear stiffness demonstrates a variety of interesting phenomena, such as sign inversion of output signal [18] and nonreciprocal wave motion [11,14,15].

Here, we model a 2D spring-mass chain system with a functional section of bilinear stiffness arranged asymmetrically. The

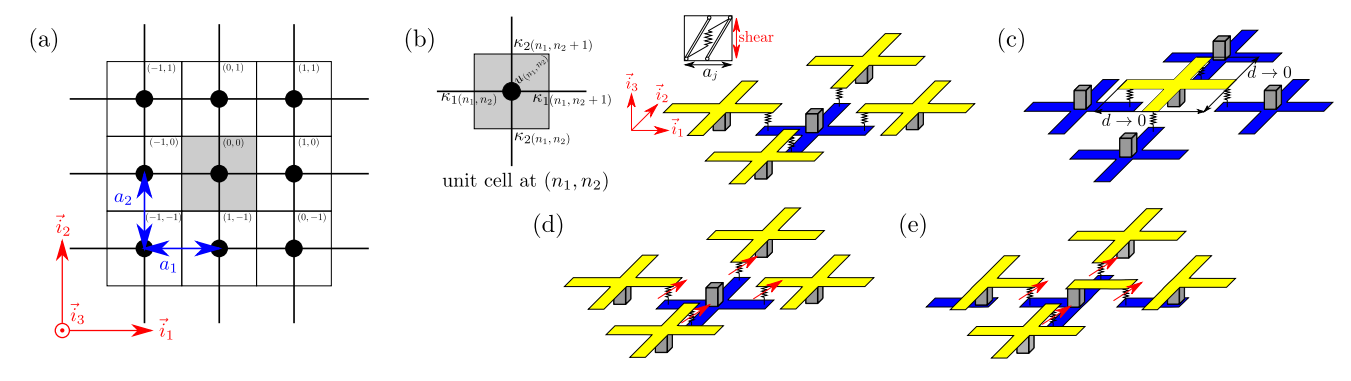


Fig. 1. 2D monatomic lattice of identical masses connected by shear springs. (a) shows the reference system  $(\vec{i}_1 \text{ and } \vec{i}_2 \text{ denote the horizontal and vertical direction, respectively); the mass displacement is in the transverse (into- and out-of-plane, labeled by <math>\vec{i}_3$ ) direction only. (b) and (c) depict the physical structure of a unit cell connecting four neighbors by linear shear springs under a spatially symmetric arrangement; the unit cell consists of a mass and a massless "+" shape structure with size  $d \to 0$ , introducing the in-plane transverse wave propagation; reciprocity prevails because the alternate pattern of "+" position maintains spatial symmetry, so that (b) and (c) stands for the state of "+" up and down, respectively. (d) all linear springs are replaced by the identical bilinear springs, and reciprocity still holds. (e) illustrates a further asymmetric modulation in horizontal  $(\vec{i}_1)$  direction by moving one leg of "+" structure in the opposite direction, resulting in the structural asymmetry of the unit cell and therefore nonreciprocity (see Eq. 5).

spatial asymmetry combined with the nonlinearity produces a significant wave scattering towards two opposite directions with direction-dependent signs of displacement. The scattering results are insensitive to driving frequency and to the relative location of the source, but depend upon the relations between the compressive and tensile stiffness of the bilinear springs and their asymmetric arrangements, refer to the detailed explanation in Fig. 7 of [15]. This nonreciprocal wave phenomenon is distinctly a two dimensional effect, which opens up the possibility of programmable scattering via flexible arrangement of spatial asymmetry.

The outline of the paper is as follows. Section 2 discusses the physical structure of the 2D lattice and the definition of spatial asymmetry; one particular case showing how waves scatter in the horizontal direction with oppositely signed offsets is demonstrated. Configurations of various spatially bilinear setups are introduced in Section 3 to show the capability of our approach to control wave directionality. A programmable waveguide in the 2D lattice consisting of several spatially asymmetric bilinear sections is proposed in Section 4. Section 5 concludes the paper.

## 2. Introduction of 2D monatomic lattice

A 2D monatomic lattice consisting of masses and springs serves as the platform for our proposed approach to achieving controllable directional wave scattering. The lattice and its structural asymmetry are discussed first. Then a fundamental configuration of a spatially asymmetric bilinear section is discussed.

#### 2.1. Lattice setup

A 2D monatomic lattice is modeled as an array of equal masses interconnected by shear springs, covering a portion of the  $\vec{i}_1$ - $\vec{i}_2$  plane, as shown in Fig. 1. Transverse (into- and out-of-plane direction,  $\vec{i}_3$ ) displacement is the single degree of freedom for the motion of each mass. Thus the springs are assumed to act in shear with a force related to the relative displacements of neighboring masses. The unit cell consists of a mass and a massless "+" shape structure (no force between them) with thickness and size  $d \rightarrow 0$ . The "+" shape structure transfers force between neighboring unit cells, leading to the transverse wave propagation within  $\vec{i}_1$ - $\vec{i}_2$  plane while neglecting rotational motion. Two states ("+" shape up and down) exist in this 2D lattice, guaranteeing the spatial symmetry (introduced later) and therefore the reciprocity of the lattice.

The periodicity of the lattice is defined by orthogonal lattice vectors  $a_1\vec{i}_1$  and  $a_2\vec{i}_2$  in the horizontal and vertical directions, respectively. The unit cell at  $n_1$   $a_1\vec{i}_1 + n_2$   $a_2\vec{i}_2$ , shown in the gray box at the center of Fig. 1(a), satisfies the equilibrium equation below (neglecting rotational motion)

$$m \ddot{u} = \sum_{i=1}^{2} \left[ \kappa_{j}^{-} \Delta u_{j}^{-} + \kappa_{j}^{+} \Delta u_{j}^{+} \right], \tag{1}$$

where  $u=u_{(n_1,n_2)}$  stands for the transverse displacement at coordinates  $(n_1,n_2)$ , and

$$\kappa_{j}^{-} = \kappa_{j(n_{1},n_{2})}, \ \kappa_{j}^{+} = \kappa_{j(n_{1}+\delta_{j1},n_{2}+\delta_{j2})},$$
(2)

with j=1 and 2 denoting the springs located along the horizontal and vertical  $(i_1$  and  $i_2)$  direction, respectively, and

$$\Delta u_i^{\pm} = u_{(n_1 \pm \delta_{i1}, n_2 \pm \delta_{i2})} - u_{(n_1, n_2)}, \tag{3}$$

representing the relative transverse displacement of two adjacent unit cells.

### 2.2. Structural asymmetry

Spatial symmetry is introduced first. Consider a unit cell, such as Figs. 1(b) and (c) show, with the same relative displacement between the unit cell and its nearest neighbors  $\Delta u_j^\pm$ . Spatial symmetry then produces the same resultant shear force,  $F_j^\pm = \kappa_j^\pm \Delta u_j^\pm$ , such that

$$\begin{cases} \Delta u_j^- = \Delta u_j^+ \\ \kappa_i^- = \kappa_i^+ \equiv \kappa_L \end{cases} \Rightarrow F_j^- = F_j^+. \tag{4}$$

j=1 when we consider the neighboring unit cells in the horizontal  $(\vec{i}_1)$  direction, and j=2 in the vertical  $(\vec{i}_2)$  direction;  $\kappa_L$  denotes the linear stiffness.

The spatial symmetry still holds in the unit cell when all linear springs are replaced by identical bilinear springs (e.g., labeled by  $\nearrow$  and the corresponding stiffness written as  $\kappa_{\nearrow}$ ) as shown in Fig. 1(d). Although the bilinear spring has different stiffnesses when compressed and stretched, two horizontally or vertically ( $i_1$ - or  $i_2$ -related) adjacent bilinear springs are always in the same condition given the same relative displacement, as Eq. 4 depicts except that  $\kappa_j^- = \kappa_j^+ \equiv \kappa_{\pm\nearrow}$ , where  $\kappa_{-\nearrow}$  stands for the compressive stiffness, and  $\kappa_{+\nearrow}$  the tensile stiffness.

In order to generate spatial asymmetry, e.g., in the horizontal  $(i_1)$  direction only, one leg in the "+" shape structure of the unit

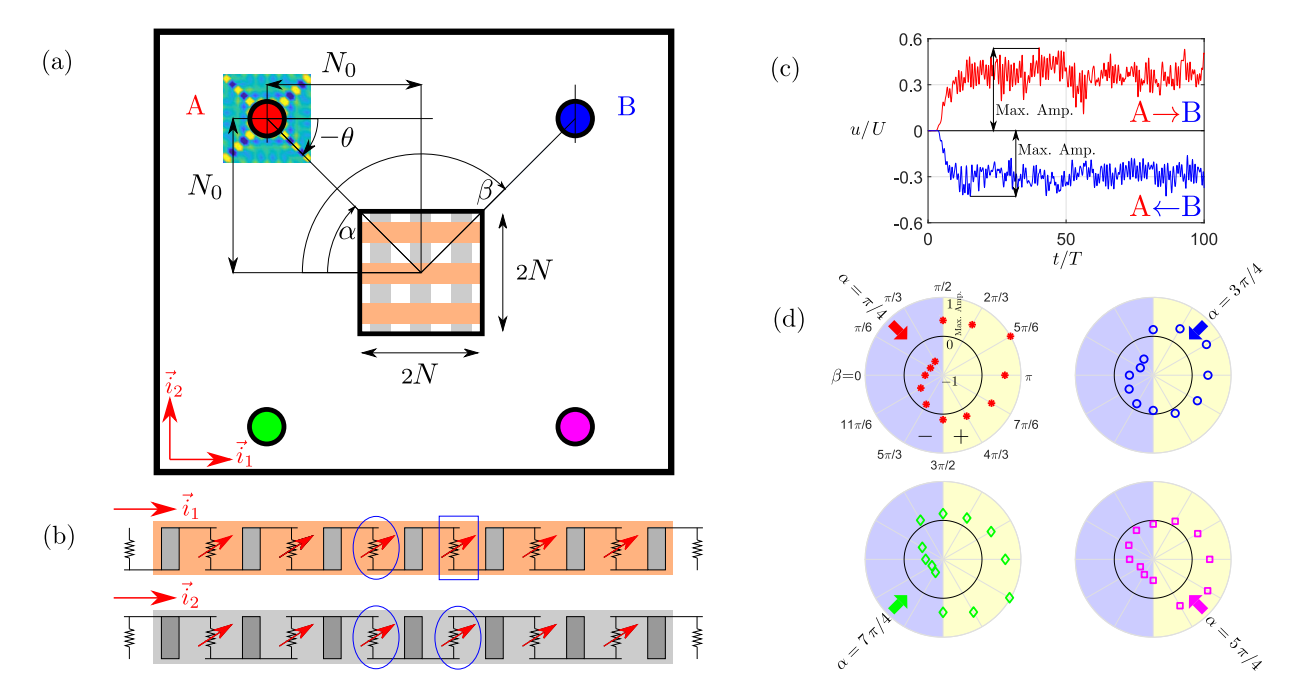


**Fig. 2.** Demonstration of directional wave scattering. (a) shows the simulation model setup: the bilinear section is square with sides of 2N bilinear springs; four potential source locations are equi-distant from the square center with  $N_0$  springs in both horizontal and vertical  $(\vec{i}_1$  and  $\vec{i}_2)$  directions, or simply represented by the angle α; the receiver is located around the square at various angles β and at the same distance to the square center as the source. The incident wave in the linear section, generated by a continuous excitation, see Eq. 6, propagates preferentially in directions  $\theta = \frac{n\pi}{4}$ , n = 1, 3, 5, 7 due to the anisotropy and dispersion of the linear system. Chains of unit cells in the bilinear section are depicted in (b): the gray shaded one represents the vertical chains (rotated 90°) consisting of symmetric unit cells connected by identical bilinear springs, while the brown shade denotes the horizontal chains of structurally asymmetric unit cells. (c) shows the dynamic responses at receivers when positions A and B are considered: a positive steady shift in displacement for incidence coming from A and negative one from B. (d) shows the consistent wave scattering. Each polar plot illustrates the maximum resultant amplitudes (refer to the labels in (c)) recorded at different locations around the square for incidence (labeled by arrows with relevant colors) from one of four directions. Together they illustrate stable scattered waves in the horizontal direction: scattering to the left results in a negative offset (markers are located within the solid black circle and the region is covered by blue) while a positive offset for right scattering (markers outside the circle and the region in yellow). (For interpretation of the references to color in this figure legend, the reader is referred to the web version of this article.)

**Table 1** The possible locations of source and receiver represented by  $\alpha$  and  $\beta$ .

α	β
$\frac{n\pi}{4}$ , $n = 1, 3, 5, 7$	$\frac{n\pi}{6}, n=0,1,\ldots,11$

cell is moved to the opposite position, up or down, see Fig. 1(e). Given the same relative displacement, the asymmetric structure results in the opposite conditions for two adjacent bilinear springs in horizontal  $(i_1)$  direction (so j=1): one is compressed and the other stretched. The asymmetric spatial structure thus results in different shear forces,

$$\begin{cases} \Delta u_1^- = \Delta u_1^+ \\ \kappa_1^- \equiv \kappa_{\mp \nearrow} \neq \kappa_1^+ \equiv \kappa_{\pm \nearrow} \end{cases} \Rightarrow F_1^- \neq F_1^+.$$
 (5)

## 2.3. Simulation model setup

Simulations are used to examine the nonreciprocal wave directionality generated by configurations of spatially asymmetric bilinearity. We consider a square section with sides of 2N springs in the purely linear lattice, see Fig. 2(a), within which a designated spatially asymmetric bilinearity is introduced. The positions of input source and receiver are set equally distant relative to the square functional section: e.g., in Fig. 2(a), the locations A and B of the source and receiver are at a distance of  $N_0$  springs in both horizontal and vertical  $(\vec{i}_1$  and  $\vec{i}_2)$  directions from the square center. For simplicity, the source and receiver positions are represented by angles  $\alpha$  and  $\beta$ , respectively. Table 1 lists all the possible positions specified by these two angles.

## 2.4. Excitation

The incident wave is generated by applying a displacement to the unit cell at the source,

$$u = \mathcal{H}(t)U\sin\omega t\,, (6)$$

where U is the input amplitude,  $\omega$  the excitation frequency, and  $\mathcal{H}$  represents the Heaviside function. Specifically, we take  $a_1=a_2=1$  m,  $\kappa_1=\kappa_2=\kappa_L=1$  N/m, m=1 kg for the model, and U=1 m,  $\omega=2$  rad/s for excitation. This choice of frequency results in wave propagation in four discrete directions,  $\theta=\frac{n\pi}{4}$ , n=1,3,5,7. The insert figure at top left in Fig. 2(a) shows the resultant spatial wavefield distribution in the linear section. This highly directional source guarantees that the receiver positions are always located in a region without direct transmission from the source.

### 2.5. Directional wave scattering demonstration

As a first case, we consider a functional section with spatially asymmetric bilinearity arranged in the horizontal  $(i_1)$  direction and with the vertical  $(i_2)$  direction bilinear but symmetric, see Fig. 2(b) and check Table 2 for stiffness values (labeled by  $\nearrow$ ). Nonreciprocal dynamic responses are evident in Fig. 2(c): a positive steady offset in time is obtained for incidence from position A, but a negative one from B; the maximum amplitudes are marked to represent the values and signs, indicating the dominant scattering directions in the top left polar plot in Fig. 2(d) (discussed later).

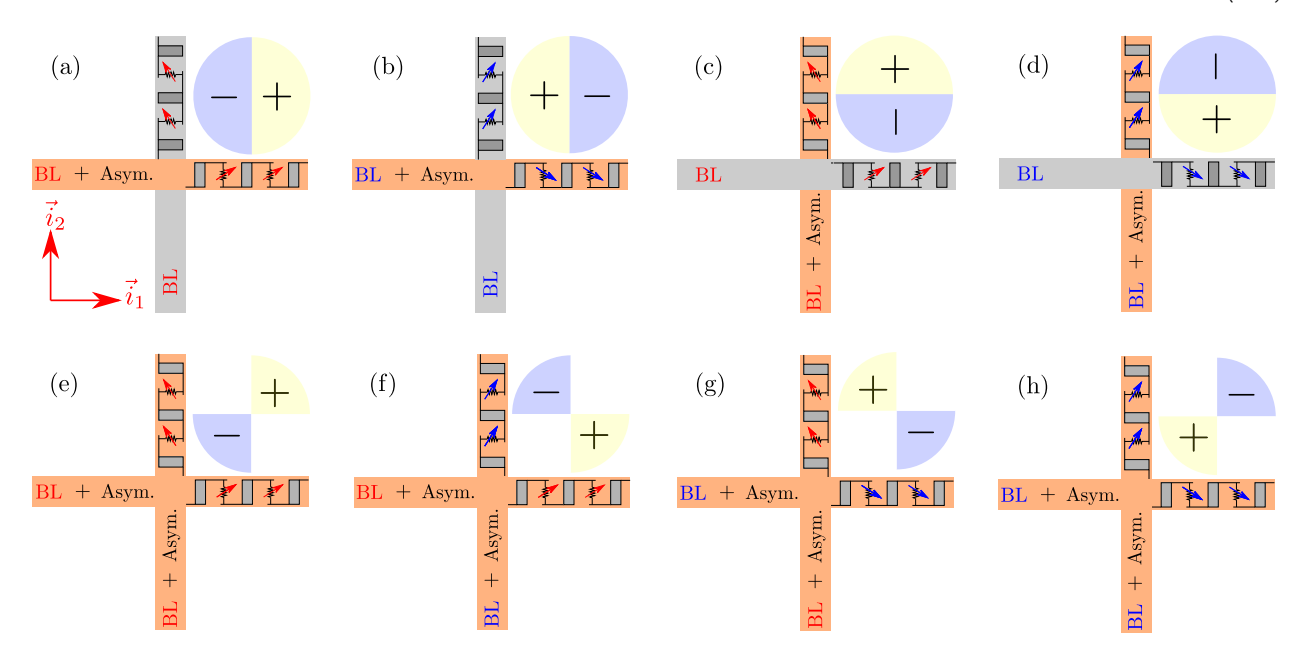


**Fig. 3.** A variety of directional wave scatterings. Each subfigure relates to a specific spatially asymmetric bilinear configuration: a cross consists of two perpendicular bars indicating the horizontal and vertical makeup of the unit cell with information on the bilinearity and asymmetric arrangement; along with a polar plot showing the simplified scattering results. (a) and (b) show the horizontal scattering of *Case 1* in Section 3 with the horizontally arranged spatial asymmetry, while (c) and (d) demonstrate the vertical scattering of the vertically asymmetry-arranged *Case 2*. The outcomes of *Case 3* with both horizontal and vertical arrangements of spatial asymmetry are demonstrated in (e) - (h), indicating a diagonal scattering.

Comprehensive scattering results are shown in Fig. 2(d). Each polar plot demonstrates an incident wave from a specific direction  $\alpha$  (labeled by an arrow with relevant color); the maximum resultant amplitudes recorded at a variety of locations (indicated by different values of angle  $\beta$ ) are marked in the polar plot. In sum, four different locations of source are applied and the dynamic behaviors at twelve positions of receiver are considered, see Table 1 for all the values of  $\alpha$  and  $\beta$  in the tests.

The four polar plots of Fig. 2(d) show similar results: scattering to the left produces a negative offset (markers are located within the solid black circle of the polar plot and the relevant semicircle is covered by blue), while scattering to the right gives a positive one (markers outside the circle and semicircle in yellow). These simulations indicate that regardless of where the incidence comes from, two distinct parts of scattered waves are observed with the oppositely signed offsets redirected in horizontally ( $\vec{i}_1$ -related) opposite directions.

#### 3. Programmable scattering

In addition to varying the bilinear stiffness, spatial asymmetry, which can be set in one direction (horizontal or vertical,  $\vec{i}_1$  or  $\vec{i}_2$ ) or both, provides another dimension of directivity control. We next explore various configurations, showing the programmable scattering control of our approach.

#### 3.1. Bilinear stiffness

For simplicity, we only consider two types of bilinear springs, labeled by  $\nearrow$  and  $\searrow$ : setting the bilinear stiffnesses  $\kappa_{\pm\nearrow}=\kappa_L\pm\Delta\kappa_\pm$  and  $\kappa_{\pm\searrow}=\kappa_L\mp\Delta\kappa_\pm$ ; equivalently, we have  $\kappa_{\pm\nearrow}=\kappa_{\mp\searrow}$ . Extreme bilinearity guarantees significant nonreciprocal displacement offsets, requiring drastic difference between tensile and compressive stiffness, e.g.  $\Delta\kappa_-\ll\Delta\kappa_+$ , see Table 2 for the set of stiffnesses considered.

**Table 2** The stiffness of linear and bilinear springs. All linear springs are identical, and the bilinear springs satisfy  $\kappa_{-\nearrow} \ll \kappa_{+\nearrow}, \kappa_{-\searrow} \gg \kappa_{+\searrow}$  and  $\kappa_{\pm\nearrow} = \kappa_{\mp\searrow}$ . The unit is N/m

$ \kappa_1 = \kappa_2 = \kappa_L $	$\Delta \kappa$	$\Delta \kappa_+$	K	$\kappa_{+}$	κ_∖_	$\kappa_{+\searrow}$
1	0.875	10	0.125	11	11	0.125

#### 3.2. Alternative spatial configurations

We first consider asymmetric bilinearity in one direction only (either  $\vec{i}_1$  or  $\vec{i}_2$ ) and then in both horizontal and vertical  $(\vec{i}_1$  and  $\vec{i}_2)$  directions. By combining spatially asymmetric arrangements with varying bilinear stiffness, a variety of directional wave scattering effects can be obtained.

## 3.2.1. Configuration 1: Bilinearity + spatial asymmetry in horizontal direction only

The types of bilinear spring and horizontal asymmetry considered are shown in Figs. 3(a) and (b), along with simplified scattering results. Similar to the observation in Section 2, comparison of Fig. 3(a) and (b) shows that switching the bilinear spring type from  $\nearrow$  to the alternative case  $\searrow$  gives horizontal  $(i_1)$  wave scattering with oppositely signed offsets, but the signs of the corresponding scattering directions are reversed.

# 3.2.2. Configuration 2: Bilinearity + spatial asymmetry in vertical direction only

Simulation results in Figs. 3(c) and (d) show, as expected, that directional scattering with opposite signs occurs in the vertical  $(\vec{i}_2)$  direction. Using springs labeled by  $\nearrow$  leads to the positive sign in the upper section and negative in the lower section; conversely, reversed scattering results with positive upper section and negative lower one are obtained with  $\searrow$  springs.

## 3.2.3. Configuration 3: Bilinearity + spatial asymmetry in both vertical and horizontal directions

In this configuration Figs. 3(e) - (h) illustrate that the directional scattering is mainly along the diagonal directions. Different

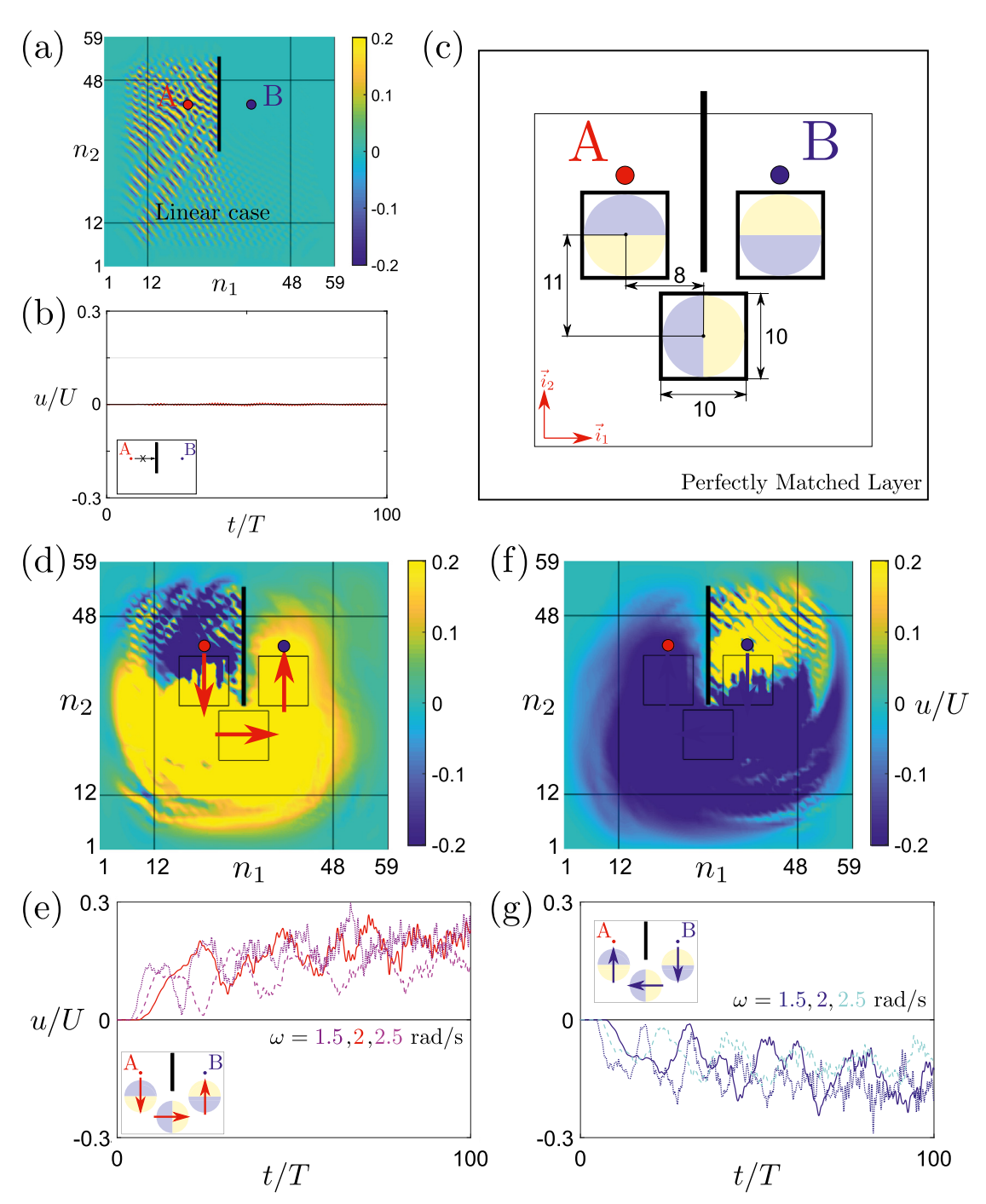


**Fig. 4.** Programmable waveguide in a 2D lattice. (a) and (b) demonstrate a purely linear case where communication between source and receiver is blocked by a barrier. (c) shows the waveguide consisting of three square functional sections, with the size, position and scattering results of each component indicated. (d) - (g) illustrate the wavefield spatial distributions ( $\omega = 2 \text{ rad/s}$ ) and dynamic responses at the receivers (various  $\omega$  values); a signal from source A (B) is guided to the receiver B (A) via multiple directional scattering, resulting in a positive (negative) dynamic offset. Multiple  $\omega$  values show similar single-signed offsets in (e) and (g), which illustrates the programmable waveguide is stable and insensitive to the driving frequency.

combinations of bilinear springs in horizontal and vertical  $(i_1$  and  $i_2)$  directions lead to unique types of diagonal scattering with opposite signs of the displacement offset. Interestingly, the diagonal scattering effect obeys the principle of superposition based on the simpler configurations with spatial asymmetry arranged in a single direction.

## 4. Application: Generation of a waveguide in a 2D lattice

The previous demonstrations of programmable wave scattering using spatially asymmetric bilinearity inspire a novel 2D waveguide design. Taking advantage of the controllable wave scattering sections, we arrange them to achieve a designated wave propagation path. Consequently, a fully controlled 2D waveguide is obtained using a passive energy-saving approach, different from active TPES-induced waveguides along the boundary of two topologically different sections.

Consider a barrier, consisting of several unit cells with displacements fixed, located between source A and receiver B in a linear 2D lattice, essentially eliminating any communication between A and B, see Figs. 4(a) and (b). By introducing three functional sections that generate directional wave scattering and

then placing them around the barrier, we can build a pathway for nonreciprocal signal transmission between A and B, see Fig. 4(c) for the sizes, relative positions and the scattering results of each introduced section.

Excitations with multiple driving frequencies (see Eq. 6)  $\omega=1.5, 2, 2.5$  rad/s are applied at positions A and B; Figs. 4(d) and (f) show instantaneous scattering results, and Figs. 4(e) and (g) demonstrate the transmitted dynamic profiles. Although different frequency values can generate a variety of wave directivities in the linear section of the monatomic lattice, refer to Fig. 2 in [15], the similarly single-signed offsets are maintained in the dynamic response as shown in Figs. 4(e) and (g), indicating that the directional scattering is insensitive to the excitation driving frequency. Under the current setup, the positive offset is related to the signal coming from position A, and the negative one from B.

#### 5. Conclusions

We have demonstrated nonreciprocity-induced wave directivity control in a 2D periodic structure consisting of masses interconnected by nonlinear shear springs. The nonreciprocity is passively achieved by spatially asymmetric arrangements of amplitude-independent bilinear springs. The directivity is insensitive to the driving frequency and the position of the forcing, and displays significantly different scattering in opposite directions with oppositely signed wave displacement offsets. The wave scattering directions and offset signs can be fully controlled and modulated by varying the values of bilinear stiffnesses and the arrangement of spatial asymmetry. Based on the programmable scattering results, a novel 2D waveguide design is proposed. The waveguide consists of multiple tailored spatially asymmetric bilinear sections in an otherwise linear 2D lattice; signals can be transmitted back and forth between two positions via this waveguide, with oppositely signed displacement offsets indicating nonreciprocal transmission. Future work could be focused on practical approaches to realizing such 2D nonreciprocal systems. Our experience is that achieving pure bilinear stiffness with low damping is difficult in practice. Despite these challenges in experimental realization, we should not overlook the potential applications of these programmable nonreciprocal systems in wave directivity design and 2D waveguide modeling.

#### **Declaration of competing interest**

The authors declare that they have no known competing financial interests or personal relationships that could have appeared to influence the work reported in this paper.

#### Acknowledgment

This work is supported by the NSF EFRI Program, USA under Award No. 1641078.

#### References

- [1] Massimo Ruzzene, Fabrizio Scarpa, Francesco Soranna, Wave beaming effects in two-dimensional cellular structures, Smart Mater. Struct. 12 (3) (2003) 363–372.
- [2] A. Spadoni, M. Ruzzene, S. Gonella, F. Scarpa, Phononic properties of hexagonal chiral lattices, Wave Motion 46 (7) (2009) 435–450.

- [3] Hussein Nassar, Behrooz Yousefzadeh, Romain Fleury, Massimo Ruzzene, Andrea Alù, Chiara Daraio, Andrew N. Norris, Guoliang Huang, Michael R. Haberman, Nonreciprocity in acoustic and elastic materials, Nat. Rev. Mater. 5 (9) (2020) 667–685.
- [4] Lisa M. Nash, Dustin Kleckner, Alismari Read, Vincenzo Vitelli, Ari M. Turner, William T.M. Irvine, Topological mechanics of gyroscopic metamaterials, Proc. Natl. Acad. Sci. 112 (47) (2015) 14495–14500.
- [5] Pai Wang, Ling Lu, Katia Bertoldi, Topological phononic crystals with one-way elastic edge waves, Phys. Rev. Lett. 115 (10) (2015).
- [6] Alexander B. Khanikaev, Romain Fleury, S. Hossein Mousavi, Andrea Alù, Topologically robust sound propagation in an angular-momentum-biased graphene-like resonator lattice, Nature Commun. 6 (1) (2015).
- [7] Anton Souslov, Benjamin C. van Zuiden, Denis Bartolo, Vincenzo Vitelli, Topological sound in active-liquid metamaterials, Nat. Phys. 13 (11) (2017) 1091–1094
- [8] R.K. Narisetti, M. Ruzzene, M.J. Leamy, A perturbation approach for analyzing dispersion and group velocities in two-dimensional nonlinear periodic lattices, J. Vib. Acoust. 133 (6) (2011).
- [9] Samuel P. Wallen, Michael R. Haberman, Zhaocheng Lu, Andrew Norris, Tyler Wiest, Carolyn C. Seepersad, Static and dynamic non-reciprocity in bi-linear structures, in: Proceedings of Meetings on Acoustics 21ISNA, Acoustical Society of America, 2018.
- [10] Itay Grinberg, Alexander F. Vakakis, Oleg V. Gendelman, Acoustic diode: Wave non-reciprocity in nonlinearly coupled waveguides, Wave Motion 83 (2018) 49–66.
- [11] Zhaocheng Lu, Andrew N. Norris, Non-reciprocal wave transmission in a bilinear spring-mass system, J. Vib. Acoust. 142 (2) (2019).
- [12] Qifan Zhang, Wei Li, John Lambros, Lawrence A. Bergman, Alexander F. Vakakis, Pulse transmission and acoustic non-reciprocity in a granular channel with symmetry-breaking clearances, Granul. Matter 22 (1) (2019).
- [13] Amir Darabi, Lezheng Fang, Alireza Mojahed, Matthew D. Fronk, Alexander F. Vakakis, Michael J. Leamy, Broadband passive nonlinear acoustic diode, Phys. Rev. B 99 (21) (2019).
- [14] Zhaocheng Lu, Andrew N. Norris, Unilateral and nonreciprocal transmission through bilinear spring systems, Extreme Mech. Lett. 42 (2021) 101087.
- [15] Zhaocheng Lu, Andrew N. Norris, Nonreciprocal and directional wave propagation in a two-dimensional lattice with bilinear properties, Nonlinear Dynam. 106 (3) (2021) 2449–2463.
- [16] S.W. Shaw, P.J. Holmes, A periodically forced piecewise linear oscillator, J. Sound Vib. 90 (1) (1983) 129–155.
- [17] Marco Scalerandi, Valentina Agostini, Pier Paolo Delsanto, Koen Van Den Abeele, Paul A. Johnson, Local interaction simulation approach to modelling nonclassical, nonlinear elastic behavior in solids, J. Acoust. Soc. Am. 113 (6) (2003) 3049.
- [18] Maria S. Kuznetsova, Elena Pasternak, Arcady V. Dyskin, Analysis of wave propagation in a discrete chain of bilinear oscillators, Nonlinear Process. Geophys. 24 (3) (2017) 455–460.
- [19] Y. Benveniste, One-dimensional wave propagation in materials with different moduli in tension and compression, Internat. J. Engrg. Sci. 18 (6) (1980) 815–827.
- [20] V.P. Maslov, P.P. Mosolov, General theory of the solutions of the equations of motion of an elastic medium of different moduli, J. Appl. Math. Mech. 49 (3) (1985) 322–336.
- [21] V.E. Nazarov, L.A. Ostrovsky, Elastic waves in media with strong acoustic nonlinearity, Sov. Phys. Acoust. 36 (1) (1990) 106–110.
- [22] L.A. Ostrovsky, Wave processes in media with strong acoustic nonlinearity, J. Acoust. Soc. Am. 90 (6) (1991) 3332–3337.
- [23] Rohan Abeyaratne, James K. Knowles, Wave propagation in linear, bilinear and trilinear elastic bars, Wave Motion 15 (1) (1992) 77–92.
- [24] S.N. Gavrilov, G.C. Herman, Wave propagation in a semi-infinite heteromodular elastic bar subjected to a harmonic loading, J. Sound Vib. 331 (20) (2012) 4464–4480.
- [25] V.E. Nazarov, A.V. Radostin, S.B. Kiyashko, Self-similar acoustic waves in homogeneous media with different-modulus nonlinearity and relaxation, Radiophys. Quantum Electron. 58 (2) (2015) 124–131.
- [26] O.V. Rudenko, Modular solitons, Dokl. Math. 94 (3) (2016) 708-711.
- [27] O.V. Rudenko, Equation admitting linearization and describing waves in dissipative media with modular, quadratic, and quadratically cubic nonlinearities, Dokl. Math. 94 (3) (2016) 703–707.
- [28] V.E. Nazarov, S.B. Kiyashko, A.V. Radostin, The wave processes in microinhomogeneous media with different-modulus nonlinearity and relaxation, Radiophys. Quantum Electron. 59 (3) (2016) 246–256.